RESWARA: Jurnal Riset Ilmu Teknik
2026, Vol. 4, No. 4, pp. 1195-1213
E-ISSN: 3025-9444

Assessment of Land Use Change Impacts on Design Flood Discharge in the Cakung Watershed Using Hydrological Modeling

Handika Putrawan [1✉], Dina P. A. Hidayat [2]
(1,2) Department of Civil Engineering and Planning, Universitas Trisakti, Jakarta, Indonesia

Abstract: *Land use land cover (LULC) change driven by urbanization in the Cakung Watershed, Jakarta, has significantly increased peak flood discharge. This study employed a quantitative approach using secondary data. LULC classification used the Random Forest algorithm in ArcGIS, applied to Landsat 5 and Landsat 8 Level 2 imagery, and the hydrological model was calibrated and validated using observed streamflow data. The watershed was divided into four sub-watersheds: Cakung Hulu–BKT, Buaran–BKT, Jatikramat–BKT, and Cakung Hilir. The study aimed to calibrate and validate the HEC-HMS model and to determine the effect of LULC change on flood discharge in the Cakung Watershed. The HEC-HMS simulation performed excellently during calibration (7 January 2024) and the first validation (11 April 2024), yielding NSE of 0.842–0.892, RSR of 0.30–0.40, and PBIAS of −1.06% to −0.78%. The second validation (4 August 2024) declined to a satisfactory level (NSE = 0.595, RSR = 0.60, PBIAS = −10.75%), yet the parameters remained reliable. LULC changes during 2000–2024 increased CN by 1%–4% and impervious area by 18%–182%, indicating reduced infiltration and expanded built-up areas, which raised design flood discharge across all sub-watersheds. Cakung Hilir produced the highest peak discharge (120.30 m^3/s), while Cakung Hulu–BKT showed the largest increase (12.89%). The results showed that higher CN and impervious area values corresponded to greater flood discharge. Therefore, LULC change is a contributing factor to increased flood discharge in the Cakung Watershed.*

Article history:
Received: 18 July 2026
Revised: 13 August 2026
Accepted: 02 September 2026
Published: 07 September 2026

Keyword:
HEC-HMS, peak discharge, land use, curve number, impervious area

How to cite: Putrawan, H., & Hidayat, D. P. A. (2026). Assessment of Land Use Change Impacts on Design Flood Discharge in the Cakung Watershed Using Hydrological Modeling. *RESWARA: Jurnal Riset Ilmu Teknik*, *4*(4), 1195–1213. https://doi.org/10.70716/reswara.v4i4.763

INTRODUCTION

Quantifying how land-use change drives design flood discharge in rapidly urbanizing tropical watersheds remains methodologically constrained, even as the underlying hazard grows more severe. Urban flooding in Jakarta represents a persistent hydrological hazard driven by the compounding effects of rapid urbanization, climatic variability, land-use transformation, and land subsidence. The city has been identified as one of the world's most vulnerable megacities to sea-level rise and to intensifying extreme-rainfall regimes (Widodo, 2017). Progressive urban expansion has encroached upon natural infiltration areas, diminishing the pervious fraction of the catchment and amplifying surface runoff generation; when coupled with climatic change, this transformation has been projected to elevate flood risk by up to 402% in 2050 (Januriyadi et al., 2018). The Cakung Watershed, which drains eastern Jakarta and its upstream reaches in Bekasi, exemplifies this trajectory, having undergone sustained conversion of vegetated land to impervious surfaces that has measurably altered its hydrological response and increased flood discharge. Robust quantification of this land-use effect, specifically, hinges on two methodological requirements that prior studies have not jointly satisfied:

✉ *Corresponding author:* ***hputrawan24@gmail.com***

temporally consistent characterization of land cover, and rigorous verification of hydrological model performance.

Land-use and land-cover (LULC) change is well established as a principal control on catchment hydrological behavior, governing infiltration, runoff generation, and peak-discharge magnitude (Suharyanto et al., 2021). Applications of the Hydrologic Engineering Center–Hydrologic Modeling System (HEC-HMS) have consistently shown that LULC change amplifies peak discharge and modifies the timing of the hydrological response to rainfall (Susilawati & Maulani Ikhsan, 2024). Reliable attribution of discharge changes to land-use dynamics, however, is contingent upon both an accurate, temporally coherent representation of land cover and a hydrological model whose predictive skill has been rigorously validated conditions inconsistently fulfilled in the existing literature.

Notwithstanding the extensive literature linking LULC change to flood discharge, three methodological gaps persist and motivate the present study. First, the majority of prior studies have relied on pre-existing secondary land-use maps rather than deriving land cover directly from satellite imagery, thereby compromising the temporal consistency of the catchment parameters estimated across observation periods. Second, the reliability of the hydrological models employed has frequently been evaluated using a single performance index, with incomplete reporting of calibration parameters or, in some cases, without calibration altogether, undermining the credibility of the reported results. Third, although machine-learning classifiers such as Random Forest have demonstrated robustness and high accuracy in classifying spectrally heterogeneous remote-sensing data (Aziz et al., 2024; Ramachandra et al., 2023), and has consistently outperformed alternative classifiers such as support vector machines and artificial neural networks in recent land-cover accuracy benchmarking on multispectral satellite imagery (Rihan et al., 2025), they have seldom been integrated end-to-end with a fully calibrated hydrological model to quantify their propagated effect on flood discharge. Collectively, these gaps underscore the need for an integrated framework that couples reproducible, machine-learning-based land-cover classification with a rigorously calibrated and validated hydrological model.

To address these gaps, the present study derives LULC directly from multi-temporal Landsat Level-2 imagery (2000–2024) using the Random Forest algorithm implemented in ArcGIS, yielding consistent and reproducible classifications for each observation period and reducing reliance on pre-existing cartographic products. The classified land cover is subsequently parameterized into Curve Number and impervious-area inputs for a HEC-HMS model, the reliability of which is assessed concurrently through three statistical criteria the Nash–Sutcliffe Efficiency (NSE), the RMSE–observations standard-deviation ratio (RSR), and the Percent Bias (PBIAS). The simultaneous application of these complementary criteria affords a more comprehensive appraisal of model performance, as the limitation of any individual metric is offset by the others (Moriasi et al., 2007).

This study's contribution lies in the rigorous, end-to-end quantification it provides for the Cakung Watershed: multi-temporal Random Forest land-cover classification (2000–2024), derived consistently across two Landsat sensor generations (Level-2 imagery), is coupled with a HEC-HMS model whose reliability is established under three concurrent statistical criteria rather than a single index. The general strategy of linking remote-sensing-derived land cover to HEC-HMS is not itself new and has been applied in other Indonesian watersheds (Pranoto et al., 2026; Supratman et al., 2024; Wahyudi et al., 2024); this study's contribution is therefore best understood as a rigorously validated, watershed-specific quantification for a previously under-studied catchment rather than a methodological innovation. What the results do add is a more specific empirical finding: Curve Number and impervious area, although both indicators of urbanization, increased at markedly different rates under the same land-use transition (1–4% versus 18–182%), indicating that impervious area is the more sensitive indicator of urbanization-driven flood response in this setting. The study thereby contributes a reproducible framework for quantifying the impact of land-use change on design flood discharge in a rapidly urbanizing tropical watershed, offering direct relevance to urban watershed management and flood-mitigation-oriented spatial planning.

The objective of this study is to calibrate and validate the *Hydrologic Engineering Center–Hydrologic Modeling System* (*HEC-HMS*) against observed discharge data in the Cakung Watershed, as well as to analyze land use changes and their impacts on design flood discharge. The findings of this study are expected to provide valuable insights for urban watershed management and support spatial planning based on flood mitigation strategies. Furthermore, this study contributes to a quantitative understanding of the relationship between land use change and flood discharge.

Watershed

Land use change significantly affects the characteristics of a watershed. Such changes, particularly the conversion of land into built-up areas, including residential areas, industrial zones, and infrastructure, alter the hydrological conditions and overall ecosystem functions of the watershed. Numerous studies have demonstrated that land use changes influence infiltration processes, surface runoff, and water quality within a watershed. One of the most prominent impacts of land conversion is the alteration of hydrological responses, which increases flood risk in areas that were previously less vulnerable to flooding.

The loss of vegetation cover is one of the primary factors influencing changes in watershed characteristics. The reduction of vegetation cover increases surface runoff, which not only elevates flood risk but also contributes to the deterioration of water quality (Crabbé & Coppens, 2019). Furthermore, inappropriate land use management, particularly in flood-prone areas, can increase watershed vulnerability to extreme weather events and hydrometeorological disasters. Both climate change and land use change are dominant determinants that alter streamflow within watersheds, so water resource policies need to account for the combined impacts of these two factors to ensure sustainable water resource management (Mahmood et al., 2024).

Land Use And Land Cover Classification

Land use change is an important factor influencing watershed hydrological responses because it directly affects runoff generation, infiltration, and flood characteristics. The conversion of natural land cover into developed areas generally increases runoff and flood potential (Suharyanto et al., 2021).

Land cover and land use data extraction from Landsat 5 Level 2 and Landsat 8 Level 2 satellite imagery in the Cakung Watershed was performed digitally using a machine learning approach through supervised learning with the Random Forest algorithm.

Machine learning (ML) is a branch of artificial intelligence (AI) that focuses on developing algorithms that enable computers to learn patterns from empirical data without being explicitly programmed for each specific task. Along with advances in computational technology, machine learning has continued to develop and has been widely applied across various fields. Through learning from available datasets, computers are capable of identifying patterns, generating predictions, and solving complex problems more effectively.

Supervised learning is one of the most commonly applied approaches in machine learning, in which a model is trained using labeled data with known target outputs. In this approach, each training dataset consists of input variables and corresponding output labels, allowing the model to learn the relationship between them and generate accurate predictions. The primary objective of this learning process is to minimize the error between model predictions and actual values through optimization techniques. Among supervised classifiers, the Random Forest algorithm has been widely adopted for land use land cover classification owing to its high accuracy and robustness in handling heterogeneous remote sensing data (Aziz et al., 2024; Ramachandra et al., 2023).

Rainfall

The rainfall used in flood discharge calculations is the rainfall that occurs simultaneously throughout the watershed. In water resources planning and flood control, the required data are not rainfall measurements from a single point, but rather the average rainfall over the entire area of interest. This value is referred to as areal rainfall and is expressed in millimeters (Widodo, 2017). The influence area of each rainfall station can be determined using the Thiessen Polygon method, which remains widely applied for gauge-based areal rainfall estimation in hydrological modeling (Nagkoulis, 2024). This method divides the watershed area into polygons based on the location of rainfall stations, where each polygon represents the area of influence of a particular station. The area proportion of each polygon is then used as a weighting factor to calculate the average areal rainfall.

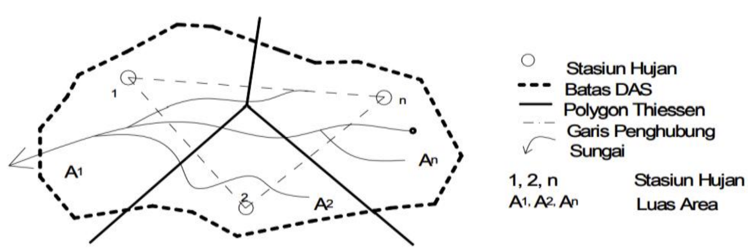

Figure 1. Thiessen Polygon Method (Limantara, 2018)

$$R = \frac{A_1 d_1 + A_2 d_2 + A_3 d_3 + \dots \dots \dots \dots + A_n d_n}{A_1 + A_2 + A_3 + \dots \dots \dots + A_n} \quad (1)$$

Rainfall Frequency Analysis

The design rainfall used in flood discharge calculations must comply with applicable standards before being applied in the hydrological analysis. The determination of design rainfall is performed through frequency analysis, beginning with the calculation of statistical parameters, followed by logarithmic statistical analysis and goodness-of-fit tests to identify the most appropriate probability distribution for the rainfall data characteristics. The design rainfall values are then obtained based on the statistical parameters derived from the analysis. In this study, the probability distributions applied include the Normal, Log Normal, Gumbel, and Log Pearson Type III distributions, as these four distributions are the most commonly used in hydrological frequency analysis and each is suited to different rainfall data characteristics, so that the most appropriate distribution can be selected through the goodness-of-fit test (Kristiawan & Irawan, 2023; Montes-pajuelo et al., 2024).

Goodness of Fit Test

The goodness-of-fit test is conducted to determine whether the selected probability distribution can adequately represent the statistical characteristics of the analyzed sample data. In this study, the goodness-of-fit analysis was performed using two methods, namely the Chi-Square test and the Kolmogorov–Smirnov test (Soewarno, 1995). Both tests remain widely applied in recent flood frequency studies to identify the best-fit probability distribution for hydrological data (Baitarani et al., 2024; Turhan, 2022). The significance level applied in this study was 5% (α = 0.05), while the degree of freedom was calculated using the following equation.

a. Chi Square Test

The goodness-of-fit test aims to determine whether the selected probability distribution equation can adequately represent the statistical distribution of the analyzed sample data. In this test, the main focus is the comparison between the observed frequency and the expected frequency within each distribution class.

$$Dk = G - R - 1 \tag{2}$$

$$G = 1 + 3,322\ Log \tag{3}$$

Description :
Dk = Degree of freedom
G = Number of distribution classes
R = Value of 2 for Normal and Binomial distributions, and value of 1 for Poisson distribution

$$X_h{}^2 = \sum_{i=1}^{G} \frac{(O_i - E_i)^2}{E_i} \tag{4}$$

Description:

$X_h{}^2$ = Calculated chi-square parameter
G = Number of distribution classes
Oi = Number of observed values in the *i*-th distribution class
Ei = Number of theoretical values in the *i*-th distribution class

b. Smirnov-Kolmogorov Test

The Smirnov–Kolmogorov goodness-of-fit test, also known as a nonparametric goodness-of-fit test, is a statistical method that does not depend on a specific distribution function. Therefore, this test does not require data grouping into interval classes; instead, it is based on a comparison between the empirical cumulative distribution and the theoretical cumulative distribution.

$$D = \text{maksimum}\ [P(X_m) - P'(X_m)] \tag{5}$$

Rainfall Intensity

Rainfall intensity is a measure of the amount of rainfall occurring within a specific period of time. It is expressed as the depth of rainfall accumulated over the Earth's surface during a given duration. In general, rainfall intensity is defined as the ratio between the total rainfall depth occurring over a certain period and the corresponding rainfall duration. The calculation of rainfall intensity is performed using the following equation (Badan Standarisasi Nasional, 2016).

$$\boldsymbol{I = \frac{R_{24}}{24}\left(\frac{24}{t}\right)^{\frac{2}{3}}} \quad (6)$$

Calibration and Validation

Each hydrological model is essentially a mathematical representation of complex natural phenomena. To ensure that the model representation corresponds to actual conditions, watershed model calibration is performed by adjusting model parameters based on observed data, allowing the model to accurately represent the hydrological response of the river system. In this study, the parameters used to evaluate the calibration performance include RSR (RMSE–Observation Standard Deviation Ratio), NSE (Nash–Sutcliffe Efficiency), and PBIAS (Percent Bias). These three metrics are widely adopted together in recent hydrological modeling studies to provide a comprehensive assessment of model performance, since the limitation of any single metric can be compensated by the others (Moriasi et al., 2007). The calculation of each parameter is performed using the following equations (USACE, 2000).

$$RSR = \frac{RMSE}{\sigma_o} = \frac{\left[\sqrt{\sum_{i=1}^{n}\left(Y_i^{obs} - Y_i^{sim}\right)^2}\right]}{\left[\sqrt{\sum_{i=1}^{n}(Y_i^{obs} - \bar{Y}_{obs})^2}\right]} \quad (7)$$

$$NSE = 1 - \left[\frac{\sum_{i=1}^{n}\left(Y_i^{obs} - Y_i^{sim}\right)^2}{\sum_{i=1}^{n}(Y_i^{obs} - \bar{Y}_{obs})^2}\right] \quad (8)$$

$$PBIAS = \left[\frac{\sum_{i=1}^{n}\left(Y_i^{sim} - Y_i^{obs}\right) \times (100)}{\sum_{i=1}^{n}(Y_i^{obs})}\right] \quad (9)$$

Description:

Y_i^{obs} = Observed data at the *i*-th observation
Y_i^{sim} = Simulated value at the *i*-th observation
$\bar{Y}_{obs}$ = Mean value of the observed data
$\bar{Y}_{sim}$ = Mean value of the simulated data
n = Total number of observations
σ = Standard deviation of observed data

Design Flood Discharge

The Soil Conservation Service Curve Number (SCS-CN) method is one of the most widely adopted approaches for estimating direct runoff from rainfall events because it integrates land use, hydrologic soil group, and antecedent moisture conditions into a single runoff parameter. Owing to its simplicity and reliable performance, the SCS-CN method has been extensively incorporated into hydrological models, including HEC-HMS, for rainfall–runoff simulation (Yoshe, 2025);(Rajesh et al., 2025).The dimensionless Soil Conservation Service (SCS) unit hydrograph is a synthetic hydrograph expressed as the ratio between discharge (q) and peak discharge (Q_p), as well as between time (t) and the time to peak discharge (time of rise, T_p). These relationships are represented by the dimensionless SCS unit hydrograph coordinates. The calculation of the unit hydrograph is performed using the following equations (Bunganaen et al., 2021).

$$qp = CA/Tp \tag{10}$$

Description:

q_p	=	Unit hydrograph peak discharge (m^3/s)
C	=	Constant value of 2.08
A	=	Watershed area (km^2)
Tp	=	Time from the beginning of rainfall to the peak flood discharge (hours)

Model HEC-HMS

Hydrological modeling is developed to represent real watershed conditions and to predict system responses before implementation in the field. A model is expected to provide predictions that closely represent actual conditions (Wahyudi et al., 2024). HEC-HMS has been widely applied in hydrological studies due to its capability to simulate rainfall–runoff processes using various precipitation loss methods, runoff transformation methods, baseflow models, and channel routing techniques. This flexibility makes HEC-HMS well suited for design flood simulation, water resources assessment, evaluation of urbanization impacts, and flood risk management (Sharu, 2021). In HEC-HMS, hydrological processes are represented through several principal components: the loss model, the transform model, the baseflow model, and channel routing. The selection of methods for each component depends on the characteristics of the watershed, the objectives of the simulation, and data availability. (Gopi & Rema, 2021). Rainfall–runoff simulation in HEC-HMS can be performed using the SCS Curve Number (SCS-CN) method for precipitation loss estimation, the SCS Unit Hydrograph method for runoff transformation, the Recession method for baseflow simulation, and the Muskingum method for channel routing (Gopi & Rema, 2021).

RESEARCH METHOD

Study Area

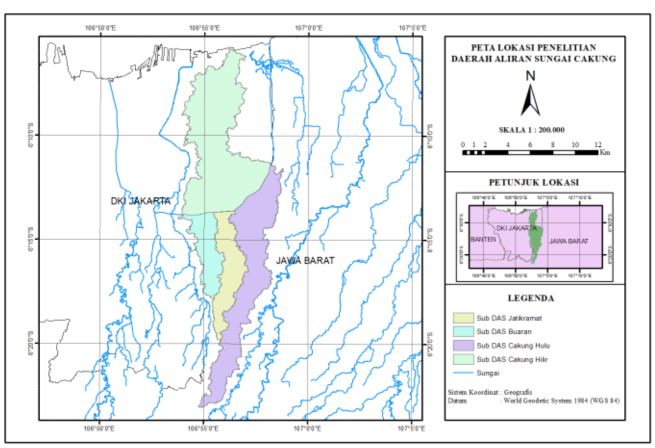

Figure 2. Study Area

The Cakung Watershed is one of the watersheds located in East Jakarta, Special Capital Region (DKI) Jakarta, with its upstream area located in Bekasi City, West Java Province. This watershed plays an important role in the water management system of eastern Jakarta, as it functions as a primary drainage system that conveys rainfall runoff, surface runoff, and wastewater from residential areas, industrial zones, and public facilities. Based on the delineation results, the Cakung Watershed has an area of 139.2 km². In this study, the Cakung Watershed was divided into four sub-watersheds.

Research Variables

Table 1. Research Variables

Nama Variabel	Definisi Operasional	Indikator / Parameter	Metode Analisis / Alat	Satuan
Independent Variable (X_1): Land Use Change	Changes in surface land utilization within the watershed that affect hydrological characteristics and surface runoff generation.	Land use and land cover classification	Supervised learning using Landsat satellite imagery in GIS	Km
		Curve Number (CN) and Impervious Area (%)	Standard SCS CN conversion table	
		Maximum potential retention (S)	SCS method equation	mm
		Initial Abstraction (Ia)	SCS method equation	mm
		Time lag (Tlag)	SCS and Snyder method equations	min
Independent Variable (X_2): Design Rainfall	The designed rainfall depth occurring over the watershed based on a specific return period.	Maximum daily design rainfall (R)	Hydrological frequency analysis (Normal, Log Normal, Log Pearson Type III, and Gumbel distributions)	mm
Dependent Variable (Y): Design Flood Discharge	The maximum surface water discharge and its occurrence time resulting from the design rainfall event.	Peak Discharge (Qp)	HEC-HMS hydrological model simulation using SCS Synthetic Unit Hydrograph method	m^3/s

The research methodology was designed in a structured and systematic manner to ensure that the analysis of the impact of land use changes on design flood discharge was conducted quantitatively and scientifically reliable. The research began with problem identification and preliminary studies to understand the hydrological characteristics and land use change patterns of the watershed through literature reviews, topographic maps, and relevant technical documents. The next stage involved the collection of secondary data, including maximum daily rainfall data from several rainfall stations, hydrological soil maps, Digital Elevation Model (DEM) data, historical flood discharge data for model calibration, and Landsat 5 Level-2 and Landsat 8 Level-2 satellite imagery.

Subsequently, land use and land cover classification was performed digitally using a supervised learning approach with the Random Forest algorithm applied to Landsat satellite imagery to generate accurate land use maps for each observation period. The spatial data were further processed using a

Geographic Information System (GIS) to determine watershed physical characteristics, infiltration parameters based on the Soil Conservation Service–Curve Number (SCS-CN) method, impervious area coverage, and time lag parameters.

Hydrological simulations were then conducted using the Hydrologic Engineering Center–Hydrologic Modeling System (HEC-HMS) by integrating various land use change scenarios obtained from the classification results and design rainfall events for different return periods. To ensure model reliability, calibration was performed by comparing the simulated flood hydrographs with secondary observed flood discharge data obtained from discharge monitoring stations.

RESULTS AND DISCUSSION

Land Use and Land Cover Classification

Land cover classification was performed using the Random Forest algorithm for four classes: Built Up Area, Water, Vegetation, and Rangeland. Training samples were collected by digitizing Regions of Interest (ROIs) as polygons, comprising a total of 1,228 training pixels (676 for Built Up Area, 340 for Water, 165 for Vegetation, and 47 for Rangeland). The classification was validated using 160 test points (40 per class) that were randomly selected and verified against 2024 Google Earth imagery, yielding an Overall Accuracy of 85.62% and a Kappa coefficient of 0.808. These values satisfy the minimum threshold of 85% recommended by Anderson et al. (2001) and indicate a strong level of agreement between the classification result and the reference data. This performance is consistent with recent benchmarking of Random Forest for multispectral land-cover mapping, which reported overall accuracies of 88.98%–91.53% and Kappa coefficients of 0.87–0.90 (Rihan et al., 2025), confirming that the classification accuracy achieved in this study falls within the range expected of a properly trained and validated Random Forest model.

The Vegetation and Rangeland classes were classified with high accuracy, whereas some confusion occurred between the Water and Built Up Area classes, as low-reflectance built-up features such as dark rooftops, building shadows, and asphalt are spectrally similar to water bodies, a confusion also widely documented in recent urban water-extraction studies using Landsat imagery and Random Forest classifiers (Song et al., 2025). This confusion, however, has a negligible effect on the subsequent hydrological analysis, since water bodies and built-up surfaces are both impervious and are represented by comparably high Curve Number values; their misclassification therefore does not materially alter the aggregated Curve Number and impervious-area parameters that serve as the primary inputs to the flood-discharge simulation. The classification result is thus considered sufficiently reliable to support the hydrological modeling undertaken in this study.

The land use analysis in the Cakung Watershed based on satellite imagery indicates a significant land conversion from natural infiltration areas into built-up areas. This change reflects the rapid expansion of urban development, which has reduced the hydrological function of the watershed and increased surface runoff.

DOI: https://doi.org/10.70716/reswara.v4i4.763

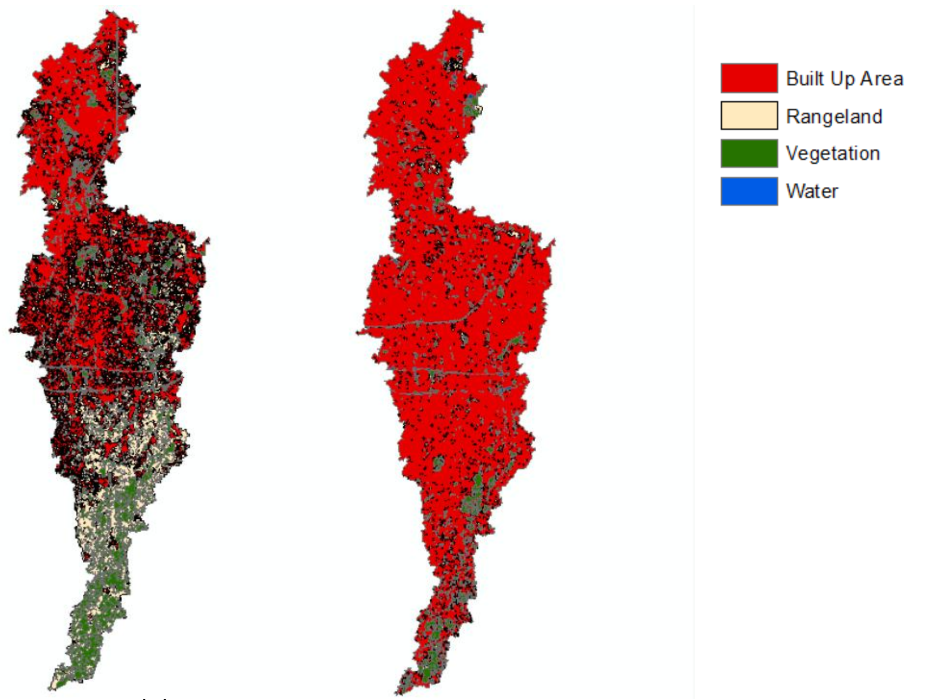

Figure 3. Land Use and Land Cover Changes in (a) 2000, (b) 2024

The land use changes from 2000 to 2024 indicate significant changes in the Cakung Watershed. As shown in the figure above, built-up areas have expanded rapidly, replacing existing open land areas. The changes in the area of each land use type within each sub-watershed are presented in the following section.

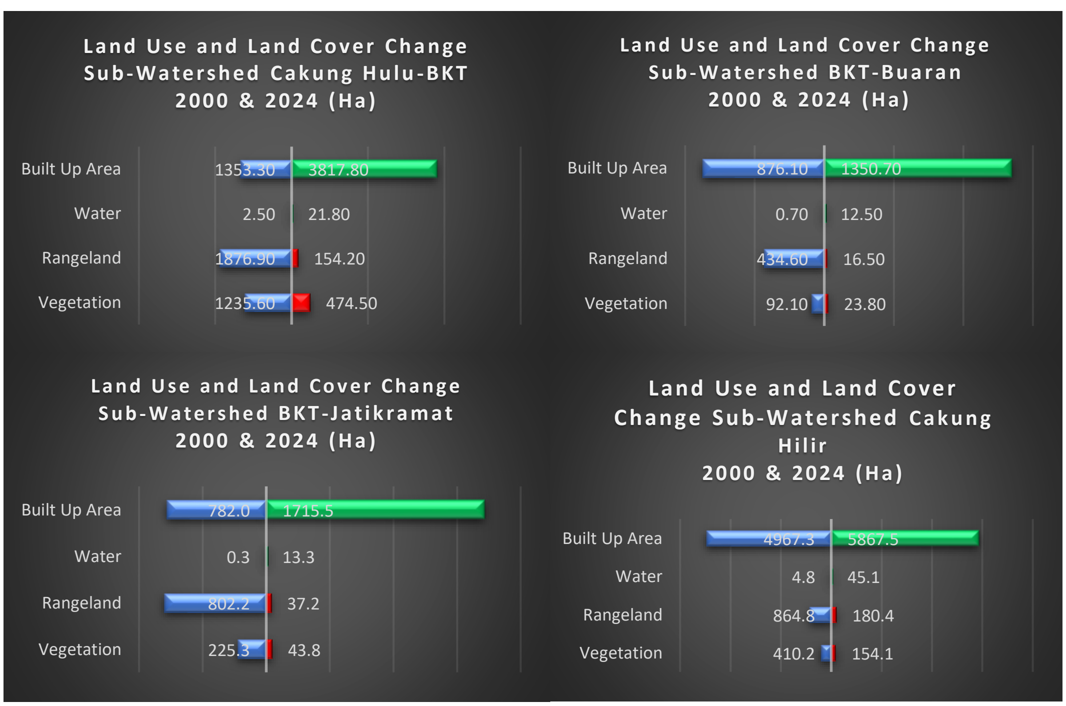

Figure 4. Land Use and Land Cover Area Distribution in Each Sub-Watershed in 2000 and 2024 (Ha)

Curve Number and Impervious Area (%)

The Curve Number (CN) values were determined based on land use classification referring to the standard Soil Conservation Service (SCS) conversion table and Hydrologic Soil Group (HSG) obtained from NASA Earthdata. The CN values were calculated using a weighted average method based on the area proportion of each land use type. The CN values and impervious area percentages for each sub-watershed are presented in the following table. During the period from 2000 to 2024, the CN values increased by 1%–4%, while the impervious area increased by 18%–182%.

Table 2. Curve Number (CN) and Impervious Area (%) Values for Each Sub-Watershed

Sub-Watershed	Parameter	Year					
		2000	2005	2010	2015	2020	2024
Cakung Hulu–BKT Sub-Watershed	Impervious area (%)	25.74	36.28	36.97	54.24	70.92	72.63
	Curve Number	84.13	84.48	86.12	87.07	87.63	87.81
Buaran–BKT Sub-Watershed	Impervious area (%)	53.06	60.46	61.35	76.45	80.66	81.80
	Curve Number	86.80	87.05	87.62	88.47	88.60	88.87
Jatikramat–BKT Sub-Watershed	Impervious area (%)	36.73	46.90	43.67	70.71	78.43	80.57
	CN	85.54	85.87	86.58	88.13	88.42	88.74
Cakung Hilir Sub-Watershed	Impervious area (%)	67.59	60.02	64.66	73.65	76.93	79.84
	CN	87.60	86.78	86.57	88.29	88.47	88.64

The increase in Curve Number (CN) across all sub-watersheds results from the conversion of pervious land cover, predominantly Rangeland and Vegetation, into built-up areas. As infiltration-promoting vegetated surfaces are replaced by developed land, the runoff potential of each sub-watershed rises, raising the composite CN, consistent with Yu & Zhang (2023), who reported that CN values increase as the impervious area of a watershed grows. In this study, however, CN and impervious area were treated as two independent parameters, so that the CN increases only modestly while the impervious area rises more sharply, since each captures the urbanization process at a different sensitivity. Impervious area exerts a disproportionately strong influence on flood discharge because paved and built-up surfaces eliminate the vertical infiltration pathway almost entirely, forcing rainfall to convert directly into surface runoff rather than being retained or slowly released as baseflow; this simultaneously shortens flow concentration time and sharpens the hydrograph peak, a mechanism similarly documented by Ongaga et al. (2024) in a 22-year assessment linking impervious-surface expansion to rising runoff in an urbanizing watershed. A comparable pattern was reported by Pranoto et al. (2026) in the Cimanceuri Watershed, Indonesia, where a 67% expansion of impervious surface area over 2013–2025 produced a corresponding rise in composite Curve Number and design discharge despite only a modest change in the CN value itself, reinforcing the finding that impervious area, rather than CN alone, is the more sensitive indicator of urbanization-driven flood response.

Areal Rainfall Analysis

In this study, areal rainfall was calculated using the Thiessen Polygon Method. This method considers the influence area of each rainfall station within the study area by assigning weighting factors based on the area of the generated polygons. Three rainfall stations were used in this study, namely Kemayoran Rainfall Station, Banten Climatology Station, and Tanjung Priok Rainfall Station. The distribution of areal rainfall based on the Thiessen Polygon Method for each sub-watershed is presented in the following table.

Table 3. Areal Rainfall for Each Sub-Watershed

Year	Areal Rainfall (mm)				Year	Areal Rainfall (mm)			
	Cakung Hulu–BKT Sub-Watershed	Buaran–BKT Sub-Watershed	Jatikramat–BKT Sub-Watershed	Cakung Hilir Sub-Watershed		Cakung Hulu–BKT Sub-Watershed	Buaran–BKT Sub-Watershed	Jatikramat–BKT Sub-Watershed	Cakung Hilir Sub-Watershed
2000	93.3	94.8	95.1	75.1	2013	162.0	193.4	190.2	143.1
2001	102.3	82.2	82.9	167.3	2014	157.4	147.9	147.0	238.5
2002	152.3	168.5	166.5	154.2	2015	171.4	177.0	175.0	223.6
2003	172.5	199.7	197.0	151.1	2016	125.5	124.5	124.8	116.6
2004	120.2	129.3	128.1	124.0	2017	153.1	179.7	176.4	159.0
2005	117.9	124.1	123.5	114.6	2018	103.3	104.6	104.0	121.2
2006	75.8	72.0	72.2	84.2	2019	92.2	90.5	90.1	117.0
2007	252.8	234.7	238.2	199.7	2020	247.3	277.5	275.2	196.3
2008	184.1	192.7	193.2	122.9	2021	99.5	94.1	94.9	92.4
2009	123.7	122.5	122.2	140.1	2022	177.3	204.0	201.3	157.9
2010	96.1	93.0	93.5	89.9	2023	91.9	79.5	80.3	116.1
2011	101.2	119.2	117.3	92.1	2024	133.8	140.9	139.8	143.0
2012	95.8	105.2	104.4	85.2					

Model Calibration and Validation

The observed discharge recorded at the Duta Kranji Water Level Monitoring Station on 7 January 2024 served as the reference for model calibration. Prior to calibration, the time lag was estimated using the SCS method (157.89 minutes), which yielded a simulated peak discharge of 10.7 m^3/s against an observed value of 6.1 m^3/s, corresponding to a Percent Bias (PBIAS) of 37.11% and a Nash–Sutcliffe Efficiency (NSE) of −1.094 and thus indicating poor agreement with the observed hydrograph. The time lag was subsequently recalculated using the Snyder method (311.11 minutes), accompanied by adjustment of the baseflow parameter. The longer Snyder lag delayed the simulated peak, aligning its timing and magnitude more closely with the observed flood peak, whereas the shorter SCS lag induced an excessively rapid hydrograph rise and overestimation of the peak. The Snyder method was therefore adopted for the subsequent design flood discharge simulations. This sensitivity of the simulated hydrograph to the choice of synthetic unit hydrograph method is consistent with comparative evaluations of Snyder, Nakayasu, and Gamma 1 in Indonesian watersheds, which likewise reported peak-discharge and time-to-peak deviations of up to several hours depending on the method selected (Ansori et al., 2023).

Following calibration, the hydrological model exhibited satisfactory performance, with all statistical indices satisfying the established criteria. The simulated peak discharge (6.0 m^3/s) closely approximated the observed value (6.1 m^3/s); the NSE improved to 0.842, categorized as very good; the PBIAS of −1.06% denoted a negligible volume error; and the RMSE–observations standard deviation ratio (RSR) of 0.40 indicated a relatively small deviation between the simulated and observed hydrographs. These results confirm that the calibrated model reliably represented the hydrological response of the watershed and was suitable for the design flood discharge analysis.

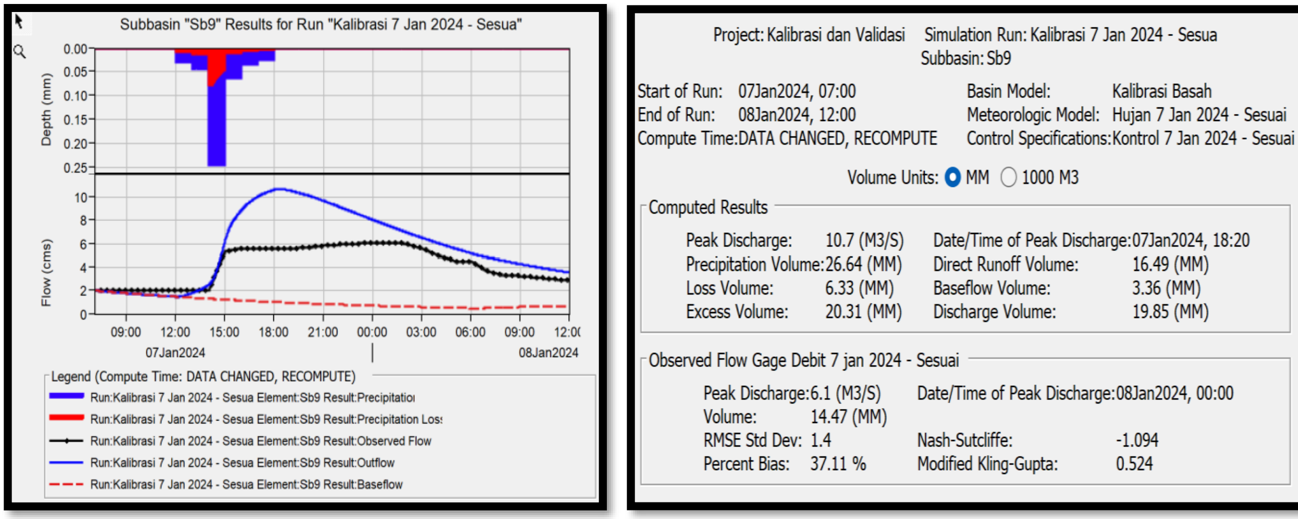

Figure 5. Uncalibrated Model Simulation Using the SCS Time Lag Method at the Duta Kranji Station (7 January 2024)

Element	Parameter	Units	Initial Value	Optimized Value
Sb9	Recession - Initial Discharge	M3/S	2	2.0000
Sb9	Recession - Ratio to Peak		0.1	0.1000000
Sb9	Recession - Recession Constant		0.1	0.25734

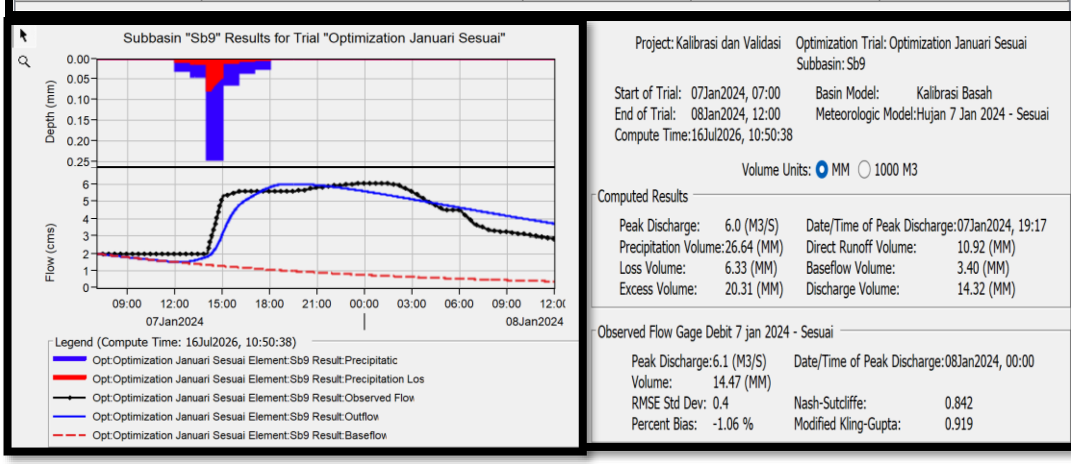

Figure 6. Flood Model Calibration at Duta Kranji Water Level Monitoring Station (January 7, 2024)

In this study, model validation was conducted using rainfall event data on April 11, 2024, and August 4, 2024. The recorded rainfall depths were 15.21 mm on April 11, 2024, and 15.19 mm on August 4, 2024. The hourly rainfall distribution for both events was developed using the Alternating Block Method (ABM).

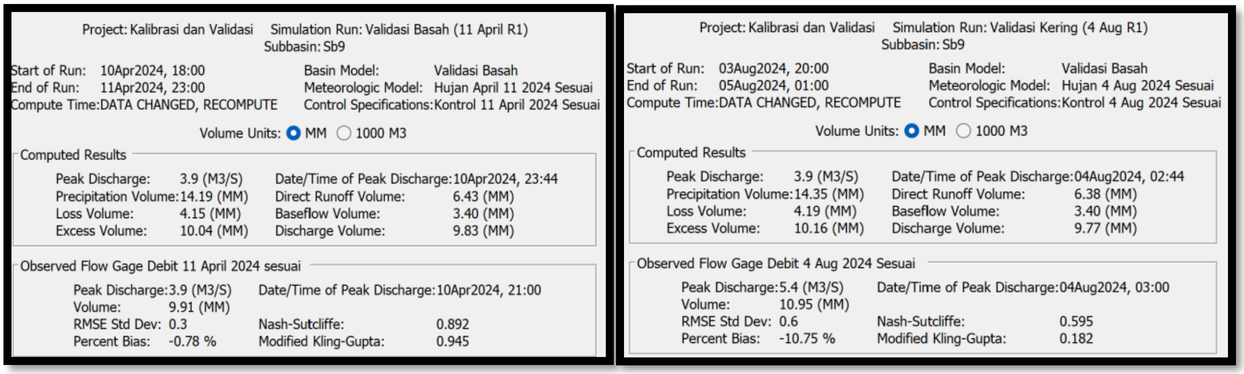

Figure 7. Flood Model Validation Results

The HEC-HMS (Hydrologic Engineering Center–Hydrologic Modeling System) modeling results for 2024 indicate that the model has good reliability and can be used for further analysis. The validation results using the rainfall event data on April 11, 2024, demonstrated very good model performance, indicated by an NSE value of 0.892, a PBIAS value of −0.78%, and an RSR value of 0.30. Meanwhile, the validation results for the rainfall event on August 4, 2024, showed satisfactory model performance, with an NSE value of 0.595, a PBIAS value of −10.75%, and an RSR value of 0.60. These results indicate that the model is still capable of representing the flood hydrograph patterns with acceptable accuracy.

Design Rainfall Analysis

Each sub-watershed within the Cakung Watershed has an area greater than 500 ha; therefore, a 25-year return period was applied for the design based on the applicable regulations (Peraturan Menteri Pekerjaan Umum Nomor 12/PRT/M/2014 Tentang Penyelenggaraan Sistem Drainase Perkotaan, 2014). The frequency analysis of design rainfall in this study was conducted using Normal, Log Normal, Gumbel, and Log Pearson Type III probability distributions.

Table 4. Goodness-of-Fit Test for Probability Distributions in Each Sub-Watershed

No.	Sub-Watershed	Probability Distribution	Chi-Square Test			Kolmogorov–Smirnov Test		
			X^2hitung	X^2Kritis	Result	Δcalculated	Δcritical	Result
1	Cakung Hulu-BKT	Gumbel Type I Distribution	15.08	7.82	Not Accepted	0.1147	0.2700	Accepted
		Normal Distribution	9.80	7.82	Not Accepted	0.1584	0.2700	**Accepted**
		Log Normal Distribution	4.04	7.82	Accepted	0.1586	0.2700	**Accepted**
		Log Pearson Type III Distribution	4.04	7.82	Accepted	0.1251	0.2700	**Accepted**
2	Buaran-BKT	Gumbel Type I Distribution	2.60	7.82	Accepted	0.0719	0.2700	**Accepted**
		Normal Distribution	4.52	7.82	Accepted	0.1515	0.2700	**Accepted**
		Log Normal Distribution	2.60	7.82	Accepted	0.1029	0.2700	**Accepted**
		Log Pearson Type III Distribution	2.60	7.82	Accepted	0.0884	0.2700	**Accepted**
3	Jatikramat-BKT	Gumbel Type I Distribution	3.56	7.82	Accepted	0.0761	0.2700	**Accepted**
		Normal Distribution	5.00	7.82	Accepted	0.1557	0.2700	**Accepted**
		Log Normal Distribution	2.60	7.82	Accepted	0.1056	0.2700	**Accepted**
		Log Pearson Type III Distribution	2.60	7.82	Accepted	0.0851	0.2700	**Accepted**
4	Cakung Hilir	Gumbel Type I Distribution	6.92	7.82	Accepted	0.0879	0.2700	**Accepted**

Normal Distribution	1.64	7.82	Accepted	0.1359	0.2700	**Accepted**
Log Normal Distribution	7.40	7.82	Accepted	0.1078	0.2700	**Accepted**
Log Pearson Type III Distribution	7.40	7.82	Accepted	0.0934	0.2700	**Accepted**

Table 5. 25-Year Return Period Rainfall for Each Sub-Watershed

No	Sub-Watershed	Design Rainfall (mm	Probability Distribution
1	Cakung Hulu-BKT	237.70	Log Pearson III
2	Buaran-BKT	273.22	Gumbel
3	Jatikramat-BKT	271.15	Gumbel
4	Cakung Hilir	243.50	Gumbel

Hourly Rainfall Distribution

Hourly rainfall data are required as input for the development of the design flood hydrograph. However, due to the limited availability of hourly rainfall data at the study area, the rainfall distribution was estimated using the Alternating Block Method (ABM), a design-hyetograph technique that derives the temporal rainfall pattern directly from the Intensity-Duration-Frequency relationship of the study area (Silveira, 2024). In this study, a 6-hour rainfall duration was applied, with the rainfall distribution determined based on the following ratios.

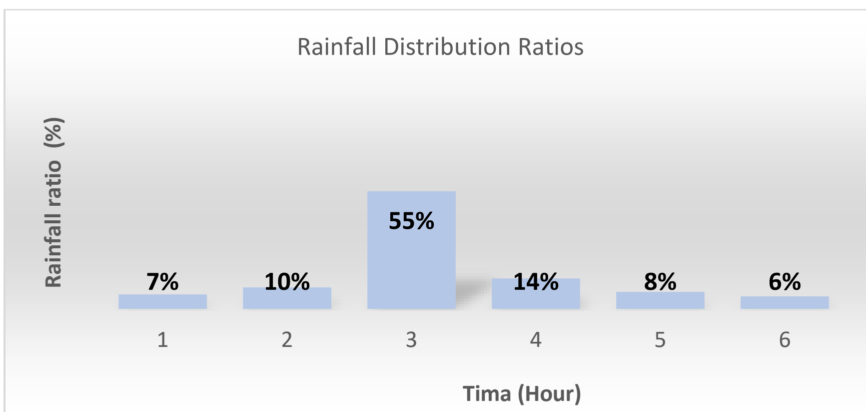

Figure 8. Hourly Rainfall Distribution Ratios Using the Alternating Block Method (ABM)

Table 6. Hourly Rainfall Distribution for Each Sub-Watershed

No	Sub-Watershed	Design Rainfall (mm)	Hour					
			1	2	3	4	5	6
			7%	10%	55%	14%	8%	6%
1	Cakung Hulu-BKT	237.70	16.03	23.85	130.81	34.00	18.99	14.02
2	Buaran-BKT	273.22	18.43	27.41	150.36	39.08	21.82	16.11
3	Jatikramat-BKT	271.15	18.29	27.21	149.22	38.78	21.66	15.99
4	Cakung Hilir	243.50	16.43	24.43	134.01	34.83	19.45	14.36

Design Flood Discharge

In this study, the design flood discharge was calculated using the HEC-HMS (Hydrologic Engineering Center–Hydrologic Modeling System) software. The rainfall–runoff transformation was simulated using the SCS Unit Hydrograph method, while the precipitation loss estimation was performed using the Soil Conservation Service–Curve Number (SCS-CN) method.

Table 7. Peak Discharge (Qp) Results for Each Sub-Watershed

No	Sub-Watershed	Peak Discharge (m^3/s) Year					
		2000	2005	2010	2015	2020	2024
1	Cakung Hulu-BKT	66.70	68.60	69.80	72.70	75.00	75.30
2	Buaran-BKT	57.40	58.10	58.30	59.70	60.10	60.20
3	Jatikramat-BKT	44.30	45.30	45.20	47.50	48.10	48.20
4	Cakung Hilir	117.60	115.70	116.50	119.10	119.70	120.30

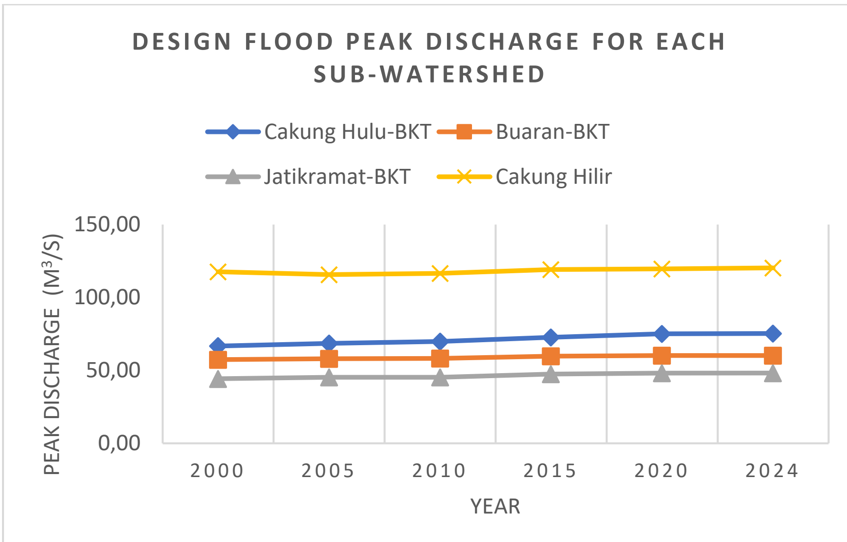

Figure 9. Comparison of Peak Discharge for Each Sub-Watershed

The hydrological analysis for the 2000–2024 period indicates an increasing trend in peak discharge across all sub-watersheds due to the reduction in surface infiltration capacity. The Cakung Hilir sub-watershed recorded the highest peak discharge, reaching 120.30 m^3/s in 2024, owing to its larger area and higher initial level of urbanization; however, its increase was the smallest (2.29%), as it was already highly urbanized at the start of the period, leaving little room for further change; this diminishing marginal effect of urbanization at already-high imperviousness levels is consistent with recent evidence that the largest relative changes in runoff occur at lower initial levels of urbanization, with the effect progressively weakening as a catchment approaches saturation (Sahraei et al., 2025). In contrast, Cakung Hulu–BKT showed the largest increase (12.89%, from 66.70 to 75.30 m^3/s), as it was initially the least developed and therefore underwent the most extensive conversion of vegetated land into built-up area. The Buaran–BKT and Jatikramat–BKT sub-watersheds exhibited intermediate increases of approximately 4% to 8%.

The increasing trend in peak discharge observed across the Cakung sub-watersheds is consistent with previous studies in urbanizing watersheds in the Jakarta region. Supratman et al. (2024) similarly reported that the expansion of urban land in the Pondok Karya watershed raised the peak discharge of the Mampang River by approximately 10% between 2002 and 2023. Likewise, a study in the

Ciliwung River Basin found that the conversion of vegetated land into built-up area progressively increased peak flood discharge, confirming that land-use change is a consistent driver of the intensifying hydrological response in Jakarta's urban catchments (Farid et al., 2022). A comparable magnitude of impervious-surface-driven discharge increase has recently been reported in other rapidly urbanizing Indonesian catchments: Pranoto et al. (2026) documented a 67% expansion of impervious area in the Cimanceuri Watershed, Tangerang, accompanied by a corresponding rise in composite Curve Number and design flood discharge, reinforcing the generality of the land-use–discharge relationship identified in the present study.

CONCLUSION

The calibration and validation results of the HEC-HMS (Hydrologic Engineering Center–Hydrologic Modeling System) model indicate that the model is capable of representing the hydrological characteristics of the Cakung Watershed. The time lag parameter calculated using the Snyder method provided a more representative result compared to the SCS method. The calibration results obtained an NSE value of 0.842, a PBIAS value of −1.06%, and an RSR value of 0.40. Meanwhile, the validation results showed very good performance for the rainfall event on April 11, 2024 (NSE = 0.892; PBIAS = −0.78%; RSR = 0.30) and satisfactory performance for the rainfall event on August 4, 2024 (NSE = 0.595; PBIAS = −10.75%; RSR = 0.60). These results indicate that the model is reliable and suitable for design flood discharge simulation in the Cakung Watershed.

Land use changes in the Cakung Watershed during the 2000–2024 period resulted in an increase in Curve Number (CN) values by 1%–4% and impervious area by 18%–182%, indicating a reduction in infiltration areas and an expansion of built-up areas. These changes contributed to an increase in design flood discharge across all sub-watersheds. The Cakung Hilir sub-watershed produced the highest peak discharge, reaching 120.30 m^3/s, while the largest increase in peak discharge occurred in the Cakung Hulu–BKT sub-watershed, at 12.89%. Higher CN and impervious area values consistently corresponded to greater peak discharge. Therefore, land use change is considered one of the contributing factors to the increase in flood discharge in the Cakung Watershed.

REFERENCES

Anderson, B. J. R., Hardy, E. E., Roach, J. T., & Witmer, R. E. (2001). *A Land Use And Land Cover Classification System For Use With Remote Sensor Data: Geological*. https://doi.org/10.3133/pp964

Ansori, M. B., Lasminto, U., & Kartika, A. A. G. (2023). Flood Hydrograph Analysis Using Synthetic Unit Hydrograph, HEC-HMS, and HEC-RAS 2D Unsteady Flow Precipitation On-Grid Model for Disaster Risk Mitigation. *International Journal of GEOMATE*, *25*(107), 50–58. https://doi.org/10.21660/2023.107.3719

Aziz, G., Minallah, N., Saeed, A., Frnda, J., & Khan, W. (2024). Remote sensing based forest cover classification using machine learning. *Scientific Reports*, 1–17. https://doi.org/10.1038/s41598-023-50863-1

Badan Standarisasi Nasional. (2016). *SNI 2415 : 2016 "Tata cara perhitungan debit banjir rencana."*

Baitarani, B., Basin, R., Singh, R., & Sananda, K. (2024). Discover Geoscience Significance of different probability distributions in flood frequency. *Discover Geoscience*. https://doi.org/10.1007/s44288-024-00072-8

Bunganaen, W., Frans, J. H., Seran, Y. A., Legono, D., & Sri, D. (2021). Rainfall-Runoff Simulation Using HEC-HMS Model in the Benanain Watershed , Timor Island. *Journal of the Civil Engineering Forum*, *7*(September), 359–368. https://doi.org/10.22146/jcef.64782

Crabbé, A., & Coppens, T. (2019). Swapping Development Rights in Swampy Land : Strategic Instruments to Prevent Floodplain Development in Flanders. In T. Hartmann, L. Slavíková, & S. McCarthy (Eds.), *Nature-Based Flood Risk Management on Private Land: Disciplinary Perspectives on a Multidisciplinary Challenge* (1st ed., pp. 85–97). Springer International Publishing. https://doi.org/10.1007/978-3-030-23842-1

Farid, M., Pratama, M. I. ;, Kuntoro, Arno Adi; Adityawan, M. B. ;, Rohmat, F. I. W. ;, & Moe, I. R. (2022). Flood Prediction due to Land Cover Change in the Ciliwung River Basin. *International Journal of Technology*, *13*(January), 356–366. https://doi.org/10.14716/ijtech.v13i2.4662

Gopi, G., & Rema, K. P. (2021). Calibration and Validation of HEC-HMS Model for Chalakudy River Basin. *International Journal of Environment and Climate Change*, *11*(5), 91–104. https://doi.org/10.9734/IJECC/2021/v11i530410

Januriyadi, N. F., Kazama, S., Moe, I. R., & Kure, S. (2018). Evaluation of future flood risk in asian megacities: A case study of Jakarta. *Hydrological Research Letters*, *12*(3), 14–22. https://doi.org/10.3178/hrl.12.14

Kristiawan, T., & Irawan, A. P. (2023). Analysis of Annual Rainfall Distribution and Planned Rain Intensity at 11 (Eleven) Rain Post Stations in Serang District. *International Journal of Entrepreneurship and Business Development*, *06*(05), 945–958. https://doi.org/https://doi.org/10.29138/ijebd.v6i5.2345.

Limantara, L. M. (2018). *Rekayasa Hidrologi* (R. I. Utami, Ed.; Revisi). ANDI.

Mahmood, S., Khan, A. U., Babur, M., Ghanim, A. A. J., Al-areeq, A. M., Khan, D., & Gamil, Y. (2024). Divergent path : isolating land use and climate change impact on river runoff. *Frontiers in Environmental Science*, *12*(February), 1–15. https://doi.org/10.3389/fenvs.2024.1338512

Montes-pajuelo, R., Rodríguez-pérez, Á. M., & López, R. (2024). Analysis of Probability Distributions for Modelling Extreme Rainfall Events and Detecting Climate Change : Insights from Mathematical and Statistical Methods. *Mathematics*, *12*, 1–24. https://doi.org/https://doi.org/10.3390/math12071093

Moriasi, D. N., Arnold, J. G., Liew, M. W. Van, Bingner, R. L., Harmel, R. D., & Veith, T. L. (2007). Model Evaluation Guidelines For Systematic Quantification Of Accuracy In Watershed Simulations. *American Society of Agricultural and Biological Engineer*, *50*(3), 885–900. https://doi.org/https://doi.org/10.13031/2013.23153

Nagkoulis, N. (2024). A genetic algorithm ' s novel rainfall distribution method for optimized hydrological modeling at basin scales Charalampos Skoulikaris. *Journal of Hydroinformatics*, *26*(6), 1295–1312. https://doi.org/10.2166/hydro.2024.224

Ongaga, C. O., Makokha, M., Obiero, K., Kipkemoi, I., & Diang'a, J. (2024). Urbanization and hydrological dynamics: a 22-year assessment of impervious surface changes and runoff in an urban watershed. *Frontiers in Water*, *6*, 1455763. https://doi.org/10.3389/frwa.2024.1455763

Peraturan Menteri Pekerjaan Umum Nomor 12/PRT/M/2014 Tentang Penyelenggaraan Sistem Drainase Perkotaan, 1 (2014).

Pranoto, W. A., Fikri, R. M., Yudianto, D., Rusli, S. R., & Wijaya, O. T. (2026). Quantifying the Role of Urban Development and Rainfall Shifts in Dynamic Hydrological Extremes. *Hydrology*, *13*(5), 123. https://doi.org/10.3390/hydrology13050123

Rajesh, G. M., Shaharudeen, S., Falah, F., & Hasher, B. (2025). Hydrological Response Analysis Using Remote Sensing and Cloud Computing : Insights from the Chalakudy River Basin , Kerala Hydrological Response Analysis Using Remote Sensing and. *Water*, *17*. https://doi.org/10.3390/w17192869

Ramachandra, T. V, Mondal, T., & Setturu, B. (2023). Relative performance evaluation of machine learning algorithms for land use classification using multispectral moderate resolution data. *SN Applied Sciences*. https://doi.org/10.1007/s42452-023-05496-4

Rihan, M., Talukdar, S., Naikoo, M. W., Shahfahad, Ansari, I., Siddiqui, A. M., & Rahman, A. (2025). Optimizing Land Use/Land Cover Mapping Accuracy: A Comprehensive Analysis of Random Forest with Explainable Artificial Intelligence Based Feature Importance Analysis. *Journal of the Indian Society of Remote Sensing*, *53*, 3735–3754. https://doi.org/10.1007/s12524-025-02229-5

Sahraei, M., McMaine, J. T., May, C. K., & Bergstrom, J. (2025). Looking Beyond MS4 Communities: Assessing Impervious Cover and Population Dynamics in Small Towns. *Journal of Environmental Management*, *380*, 124996. https://doi.org/10.1016/j.jenvman.2025.124996

Sharu, E. H. (2021). Development of HEC-HMS Model for Flow Simulation at Dungun River Basin Malaysia. *Advances In Agricultural And Food Research Journal*, *2*(January 2021), 1–16. https://doi.org/https://doi.org/10.36877/aafrj.a0000169

Silveira, A. L. L. da. (2024). Universal Equations for Rainfall Distributions from SCS and Huff Methods. *RBRH*, *29*, e23. https://doi.org/10.1590/2318-0331.292420230093

Soewarno. (1995). *Hidrologi Aplikasi Metode Statistik untuk Analisa Data: Jilid 1* (Jilid 1, Number August). NOVA.

Suharyanto, A., Devia, Y. P., & Wijatmiko, I. (2021). Floodway design affected by land use changes in an urbanized area. *Journal Of Water And Land Development*. https://doi.org/10.24425/jwld.2021.137120

Supratman, M., Kusuma, M. S. B., Cahyono, M., & Kuntoro, A. A. (2024). Flood Hazard Assessment Due to Changes in Land Use and Cover. *Civil Engineering Journal*, *10*(12), 3874–3891. https://doi.org/10.28991/CEJ-2024-010-12-04

Susilawati, T., & Maulani Ikhsan. (2024). Analisis Perubahan Tata Guna Lahan Terhadap Debit Air. *Jurnal TAMBORA*, *8*(1), 11–18. https://doi.org/10.36761/tambora.v8i1.3506

Turhan, E. (2022). An Investigation on the Effect of Outliers for Flood Frequency Analysis : The Case of the Eastern Mediterranean Basin , Turkey. *Sustainability*. https://doi.org/https://doi.org/10.3390/su142416558

USACE. (2000). *Hydrologic Modeling System Technical Reference Manual* (Number March).

Wahyudi, E., Juwono, P. T., Sholichin, M., & Suhartanto, E. (2024). Impact of Land Use Change on Flood Inundation Areas. *Journal of Hunan University (Natural Sciences)*, *51*(6). https://doi.org/10.55463/issn.1674-2974.51.6.19

Widodo, A. (2017). Analyzing Indonesia's NCICD Project to Stop the Capital City Sinking. *Otoritas : Jurnal Ilmu Pemerintahan*, *7*(2), 54–66. https://doi.org/10.26618/ojip.v7i2.769

Yoshe, A. K. (2025). Advances in Environmental and Engineering Research Sustainable Water Management Using Rainfall-Runoff Modelling in Rift Valley Basin , East Africa. *Advances in Environmental and Engineering Research*, *6*(1). https://doi.org/10.21926/aeer.2501003

Yu, X., & Zhang, J. (2023). The Application and Applicability of HEC-HMS Model in Flood Simulation under the Condition of River. *Water*, *15*(12), 2249. https://doi.org/10.3390/w15122249